DESIGN AND EXPERIMENT OF A PNEUMATIC-CYCLE PEANUT SHELLING MACHINE WITH CYLINDRICAL BEATERS

/

圆柱打板气力循环式花生脱壳机的设计与试验

Wentao SUN[1)], Jiandong YU *[1)], Yanfen LIU [1,2)], Xiaodong TAN [1)], Nan TANG [1)], Li HOU [1)]

[1)]Qingdao Agricultural University/ China

[2)] Collaborative Innovation Center for Shandong's Main crop Production Equipment and Mechanization/ China

Tel: +86 15063959335; E-mail: yjdlyf@163.com

Corresponding author: Yu Jiandong

DOI: https://doi.org/10.35633/inmateh-77-96

Keywords: *Peanut Shelling, Discrete Element Simulation, Low-damage Shelling, Design and Experiment*

ABSTRACT

To address the issue of high damage rates during the operation of peanut shelling machines, a low-damage peanut sheller was designed. This machine effectively reduces damage while improving shelling efficiency. The mechanism and working principles of the device are elaborated, and the critical shelling components are designed based on theoretical and mechanical analysis. The shelling process was simulated using Edem simulation software. Additionally, a quadratic orthogonal composite design experiment was developed using Design Expert to determine the optimal parameters. The final configuration, with a primary shelling drum speed of 302 r/min, a primary concave sieve gap of 10 mm, and a secondary concave sieve gap of 8 mm, achieved a shelling efficiency of 98.28% and a pod damage rate of 4.93%, outperforming industry standards. Field tests showed minimal discrepancy between experimental and simulation results.

摘要

针对花生脱壳机作业时花生损伤率过高的问题，设计了一种能够降低破损率的花生脱壳机，其能够实现在降低破损率的同时能够有效的提高破壳效率的破壳装置，阐明了装置的机构和工作原理，通过理论及受力分析对关键的破壳装置进行设计，采用 Edem 仿真软件对其脱壳进行模拟，以及通过 design expert 设计了二次正交组合设计实验，确定了装置的最终参数为一次脱壳滚筒转速为 302r/min,一次脱壳凹版筛间隙为 10mm,二次脱壳凹版筛间隙为 8mm 时，花生脱净率为 98.28%，花生荚果破损率为 4.93%，优于行业标准，最后通过对田间实验发现结果与仿真结果差异较小。

INTRODUCTION

Peanuts are an important economic crop in China, with a planting area of approximately 4.8 million hectares and a total production of 19.23 million tons in 2023, accounting for 17% of the global peanut output (*National Bureau of Statistics, 2024*). The shelling process significantly influences their economic value. However, conventional shelling machines are often characterized by low efficiency, high damage rates, and substantial energy consumption. In response to these challenges, researchers have conducted extensive studies both domestically and internationally. In China, a systematic classification of sheller types was conducted (*Shang et al., 2004*), and a quantitative model relating beater linear speed to working clearance was established (*Wang et al., 2004*). Recent advancements have focused on innovative mechanical designs, such as the development of a low-damage flexible comb-brush stripping device (Wang et al., 2023) and a centrifugal-axial flow combined shelling device to enhance efficiency (*Chen et al., 2022*). Concurrently, simulation techniques have been refined, including the application of advanced bonded-particle models to analyze the impact shelling process (*Liu et al., 2024*). A "three-stage" damage theory and corresponding damage reduction strategies were proposed (*Hu et al., 2010; Hu et al., 2016*). A physical property database for peanuts was established and the Discrete Element Method (EDEM) was applied for simulation and optimization (*Xie et al., 2016*). Response surface methodology was utilized to optimize process parameters (*Peng et al., 2011*). Specialized beater materials were developed to reduce damage (*Wang et al., 2015*), and a gradually spaced bar concave structure was designed to enhance separation efficiency (*Chen et al., 2014*). Parameters of beater components were optimized (*Zhang, 2013*), and the cleaning device was improved (*Li, 2018*). Performance tests on specific sheller models were conducted (*Sun et al., 2007*), while the effects of mechanical and material factors were systematically analyzed (*Lian et al., 2003*).

Internationally, a system engineering approach for post-shelling operations was proposed (*Butts et al., 2016*). A moisture detection device was developed (*Kandala et al., 1990*), and a spectral imaging-based quality monitoring system was created (*Dowell et al., 1998*). An accurate discrete element model was established (*Li et al., 2020*), and intelligent matching of shelling parameters was achieved (*Zhang et al., 2021*). Building on previous research, this study introduces cylindrical beaters to replace traditional structures and incorporates a pneumatic recycling system for secondary shelling. Through mechanical analysis, simulation, and orthogonal experiments, optimal parameters were determined. Field tests have confirmed that this design improves shelling efficiency and reduces damage rates, offering a theoretical foundation for the optimization of peanut shelling equipment.

WHOLE MACHINE STRUCTURE AND WORKING PRINCIPLE

Overall structure

Due to varying growth conditions in actual production, peanuts develop into pods of different sizes. This design needs to ensure a reduction in shelling damage while maintaining shelling completeness. In this design, traditional flat beaters were replaced with cylindrical beaters. Simultaneously, a device utilizing a fan to assist in cyclic shelling was added to the machine. This helps achieve cyclic shelling for peanuts of different sizes, better ensuring minimal damage and maintained shelling efficiency. The overall machine diagrams are shown in Figures 1.

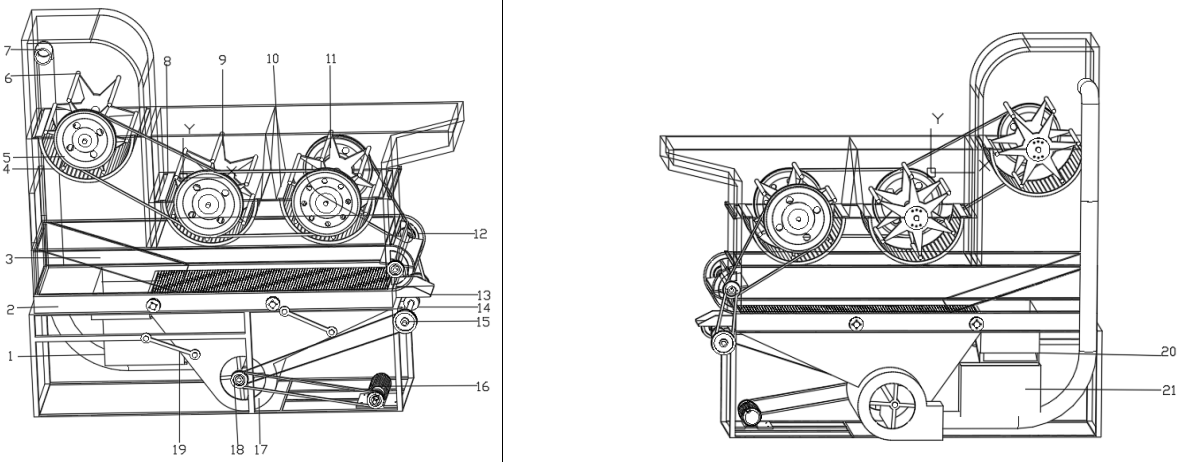

Fig. 1 – Peanut sheller overall structure schematic

1 Secondary shelling air delivery pipe; 2. Vibrating screen; 3. Secondary shelling feed baffle; 4. Secondary shelling concave sieve; 5. Secondary shelling pulley; 6. Secondary shelling beater; 7. Secondary shelling discharge outlet; 8. Primary shelling concave sieve 1; 9. Primary shelling beater; 10. Primary shelling feed baffle; 11. Primary shelling beater 2; 12. Cleaning fan 1; 13. Discharge outlet; 14. Vibrating screen connecting rod; 15. Connecting rod pulley; 16. Motor; 17. Cleaning fan 2; 18. Fan 2 pulley; 19. Fixing rod; 20. Primary shelling discharge outlet; 21. Primary shelling collection port

Working Principle

Upon activation of the sheller, peanuts are introduced through the inlet hopper and undergo initial shelling via extrusion by the primary beaters. Larger pods are effectively shelled at this stage, while smaller pods and shelled kernels proceed to the vibrating screen for separation. Unshelled small pods are pneumatically conveyed by the fan to the secondary shelling unit. Shelled kernels pass through the screen mesh and are discharged under combined vibration and airflow, during which residual shells are removed by the upper cleaning fan. The remaining unshelled small pods are transported via an air duct to the secondary shelling device, where a narrower concave sieve gap and higher drum speed ensure complete shelling. The resulting kernels are redirected to the vibrating screen for sorting, and any remaining unshelled materials are recirculated. This process continues iteratively until all peanuts are fully shelled, thereby completing the operation.

MATERIALS PROPERITY ANALYSIS

Material properties analysis

Peanut shells, as the research object, are primarily composed of cellulose, hemicellulose, and lignin. The physical structure of peanut shells is complex with a certain fibrous arrangement and porous structure. Peanut shell diagrams are shown in Figures 2 and 3.

Fig. 2 – Peanut shell front view

Fig. 3 – Peanut cross-sectional view

Taking the Qinghua Y14 peanut variety as an example, to establish a simulation model, vernier calipers were used to measure the dimensions of 100 pods. The results showed that the length is approximately 35 mm, the diameter is about 15 mm, and the shell thickness ranges from 0.3 to 0.5 mm. For modeling purposes, the dimensions were provisionally set as follows: length 35 mm, diameter 15 mm, and thickness 0.4 mm. The distribution graphs of peanut length and diameter are shown in Figures 4 and 5.

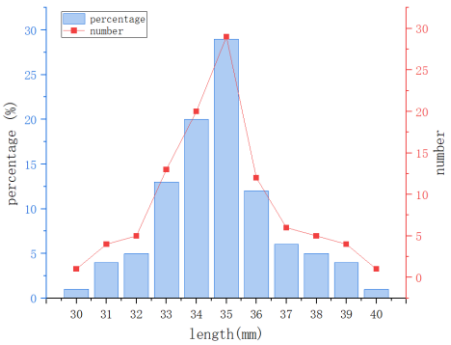

Fig. 4 – Peanut length distribution chart

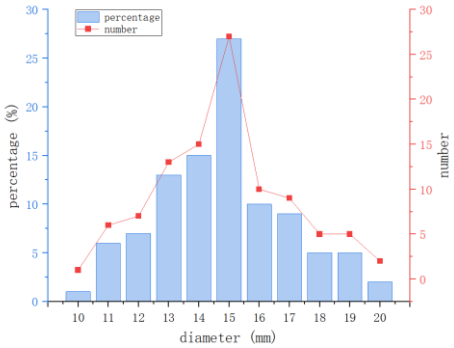

Fig. 5 – Peanut diameter distribution chart

Peanut shell is a bio-based material with good physical and mechanical properties. Studies show that the elastic modulus of peanut shells generally ranges from 2000 to 4000 MPa, and the yield strength is typically 30 to 60 MPa. Its compressive strength can reach 60 to 80 MPa (*Bassyouni et al., 2015*), and peanut shells have high fracture toughness, which gives them good toughness under impact and bending loads.

To obtain peanut shear data, compression experiments were conducted in three directions (frontal, lateral, vertical) on peanuts using a universal mechanical tester. The peanut variety Qinghua Y14 was used, and moisture content was controlled using an electronic dryer, keeping it roughly between 10% and 22%. The experimental process is shown in Figures 6-8.

Fig.6 – Frontal compression

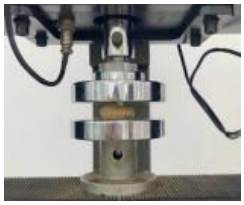

Fig. 7 – Lateral compression

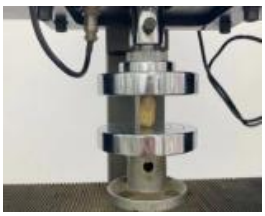

Fig. 8 – Vertical compression

The obtained data is shown in the experimental process in Figure 9.

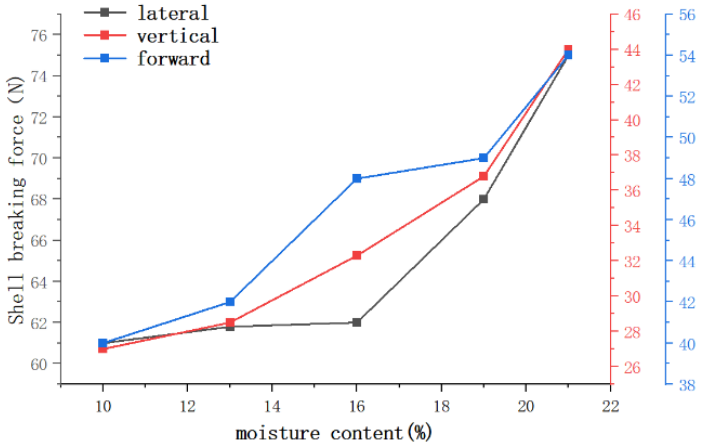

Fig. 9 – Force diagram for different peanut orientations

The force required for single peanut shell breaking was recorded. The results indicate that for the Qinghua Y14 peanut variety, the shelling force follows the order: lateral > frontal > vertical, with the vertical direction requiring the smallest force (verified by one-way ANOVA, $p < 0.05$). The average shelling force was approximately 40 N (variance≈ 64 N^2). Furthermore, compression tests on kernels with different moisture contents showed that kernels with 10% moisture content had a damage force of about 60 N (variance ≈ 144 N^2). Data on the mechanical properties of peanut shells from relevant literature provide support for subsequent stress intensity simulations based on the finite element method.

Theoretical analysis

The replacement of traditional flat beaters with cylindrical beaters is theoretically justified by their continuous curved surface, which ensures uniform force distribution during shelling—effectively minimizing localized stress concentration and reducing kernel damage. This design offers superior adaptability to natural variations in peanut size and shape through consistent surface engagement, enhancing operational stability. Mechanically, the cylindrical geometry disperses impact forces over a larger area, not only improving shelling efficiency but also mitigating mechanical wear and extending equipment service life.

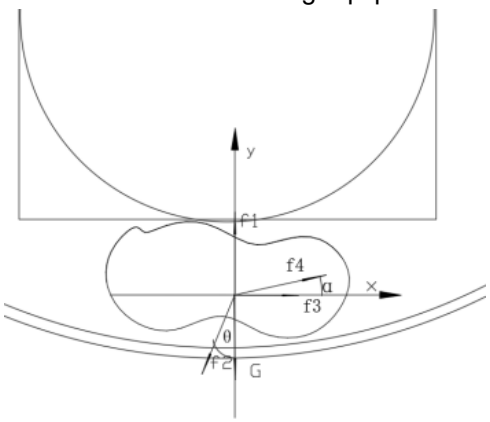

Fig. 10– Force analysis of peanut between cylindrical beater and concave sieve

Figure 10 shows the force analysis diagram of a peanut being compressed between the concave sieve and the cylindrical beater.

The force equations are as follows:

$$\sum x = f_2 \sin\theta + f_3 + f_4 \cos\alpha = 0 \tag{1}$$

$$\sum y = f_1 - f_2 \cos\theta + f_4 \sin\alpha - G = 0 \tag{2}$$

α - angle between f_2 and the y-axis, [°];

β - angle between the friction force and the horizontal direction, [°];

f_1 - support force from the concave sieve on the peanut, [N];

f_2 - support force from the cylinder on the peanut, [N];

f_3 -centrifugal force, [N];

f_4 - friction force from the cylinder on the peanut, [N];

G - peanut gravity, [N];

$$\begin{cases} f_3 = m\omega^2 r \\ f_4 = \mu f_2 \end{cases} \tag{3}$$

Combining equations (1) and (2), (3) yields:

$$f2 = \frac{G - f1}{cos\theta + \mu sin\alpha} = \frac{mg - f1}{cos\theta + \mu sin\alpha} \tag{4}$$

Compared to the traditional beater, where α is the fixed angle between the beater plate and the vertical

direction, and β is zero. The force analysis is shown in the figure 11:

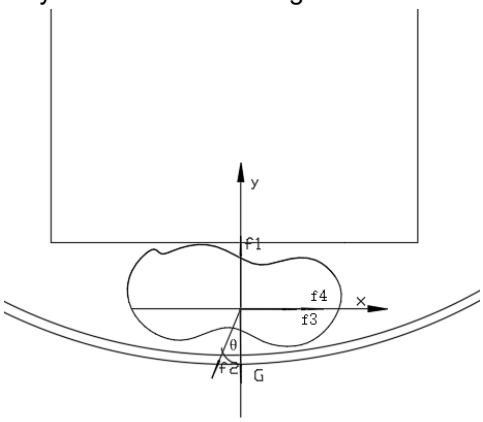

Fig. 11 – Force analysis of peanut between flat beater and concave sieve

Thus, it can be known that when the beater is changed to a flat plate, the value of α become to be '0', so the value of f_2 flat becomes larger, meaning the force the flat plate exerts on the peanut also becomes larger, making the peanut more susceptible to damage.

Simultaneously, when using a flat plate beater, the contact between the flat plate and the peanut is line contact. The contact area between the peanut and the flat plate is smaller. According to the formula:

$$\sigma = \frac{N_2}{A} \tag{5}$$

N_2 - Force from the beater on the peanut, [N]; A - Contact area between the beater and the peanut, [mm²].

The cylindrical beater offers distinct advantages over traditional flat designs by providing larger contact area with peanut pods, thereby reducing localized stress and minimizing kernel damage. This design approach is supported by thin shell theory (*Lopes et al, 2011*) which provides the mechanical basis for analyzing peanut shell failure. According to this theory, peanut shells under external compression experience progressively increasing stress until reaching instability and rupture. Stress concentration occurs primarily at the load application point, with crack propagation initiating from this center and extending outward until complete shelling occurs.

The beater was developed considering peanut dimensional characteristics and feeding requirements. Measurements were conducted on dryer-processed peanuts at 10% moisture content to establish appropriate parameters. The concave sieve clearance was specifically engineered to ensure effective primary shelling of large pods while directing unshelled small pods to the secondary shelling unit. This configuration also facilitates the passage of both large and small kernels through the sieve for subsequent processing. The clearance between beater and concave sieve was systematically optimized based on actual shelling performance and damage rates, with detailed parameters provided in Tables 1 and 2.

Table 1

Beater specific design parameters

Component	Cylindrical Beater Length / mm	Cylindrical Beater Radius / mm	Concave Sieve Gap / mm	Drum Length / mm	Drum Diameter / mm	Shelling Gap / mm
Primary Beater Assembly	548	4	10	608	300	15
Secondary Beater Assembly	548	4	8	608	300	10

Table 2

Measurement table for different sized peanut pods (Qinghua Y14)

Qinghua Y14	Single Pod Mass / g	Pod Diameter / mm	Kernel Diameter / mm
Large Pod	3.2	16	9.5
Small Pod	2.1	10	7.3

SIMULATION ANALYSIS BASED ON EDEM

Through preliminary literature review and force analysis research, using simulation experiments to study and design peanut shelling devices has become a recent research hotspot. Therefore, innovation and research on beater-type peanut shellers require simulation software for preliminary verification of the designed device, providing a theoretical basis for our innovative design. Simultaneously, by comparing simulation results with actual field experiment results, peanut breakage situation and the feasibility of the designed device can be analyzed.

Finite element model construction

Based on established dimensional parameters, a high-fidelity peanut model with realistic surface morphology was developed using SolidWorks' Power Surfacing plugin to overcome conventional modeling limitations. The model then underwent shelling simulation to isolate the exocarp structure (Figures 12-13), providing an accurate foundation for subsequent mechanical analysis of shell failure behavior.

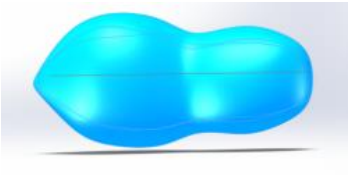

Fig. 12 – Peanut model

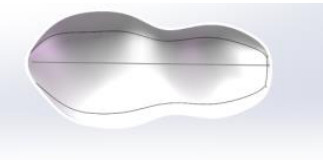

Fig. 13 – Peanut shell mode

Simultaneously, consulting literature indicates that peanut material is similar to wood, belonging to brittle material. Therefore, the brittle cracking strength criterion was adopted for the peanut shell, resulting in the following table:

Table 3

Peanut mechanical parameters

Elastic Modulus MPa	Poisson's Ratio	Density kg/m^3
15	0.3	1.4

Having completed the stress analysis of the peanut, EDEM simulation analysis was conducted. Using EDEM allows intuitive observation of the force situation and motion trajectory of peanuts within the device. EDEM can help simulate the actual situation of objects intuitively and clearly, playing an important role in this experiment. The specific simulation process and parameter values are shown below.

Peanut model filling

The peanuts were filled using the method illustrated in Figs. 14 and 15. During the filling process, a grid consisting of 31 particles in the x-direction, 63 particles in the y-direction, and 30 particles in the z-direction was employed. The corresponding filling results are shown in the accompanying figure.

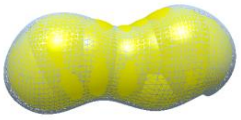

Fig. 14 – Peanut filling model

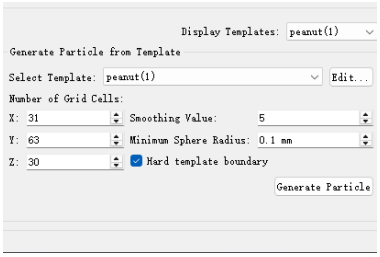

Fig. 15 – Peanut filling parameters diagram

After peanut filling was completed, the shear modulus, density, and Poisson's ratio of the particles were determined by consulting literature, making the particle parameters roughly the same as real peanuts. Parameters for the shelling device were also determined. Since shellers are mostly made of Q235A steel, steel parameters were used for the device design. Meanwhile, since contacts exist between peanut-peanut and peanut-steel, these also needed definition in the simulation. Considering the specific contact types and consulting literature, the Hertz-Mindlin contact model was chosen. Specific parameters are shown in Table 4.

Table 4

Peanut simulation parameters

Material	Peanut	Steel
Density（kg/m^{-3}）	2.50	7.89
Poisson's Ratio	0.32	0.27
Shear Modulus（MPa)	7	8250
Collision Restitution Coefficient	0.138	0.37
Static Friction Coefficient	0.63	0.35
Rolling Friction Coefficient	0.01	0.07

Note: The restitution coefficient for peanuts is for peanut-peanut contact. The coefficients for steel are for steel-peanut contact.

Device particle filling and parameter design

The device geometry was saved as an STL file and imported into EDEM. A particle factory was then created above the sheller housing. Particles were introduced into the device through the feed inlet of the shell-cracking machine at a feed velocity of 1 m/s. In actual shelling, the feed rate needs control. Therefore, a single-factor comparative experiment was used, comparing flat beaters and cylindrical beaters to observe the force on peanuts. Only the filling time needed to be controlled to be the same for both simulations, tentatively set to 4.5 seconds. Gravity acceleration was added. Since only the force on the peanuts needed simulation, a simple sheller housing was added around the beaters to simulate the external environment, ensuring simulation reliability. The beater design is illustrated in Figure 16.

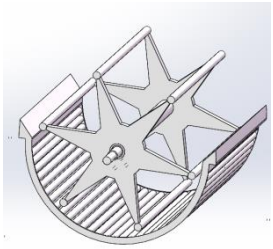

Fig. 16 – Cylindrical beater schematic diagram

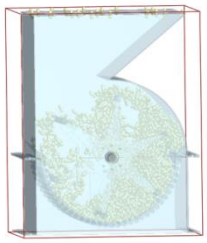

Fig. 17 – Peanut particle filling diagram

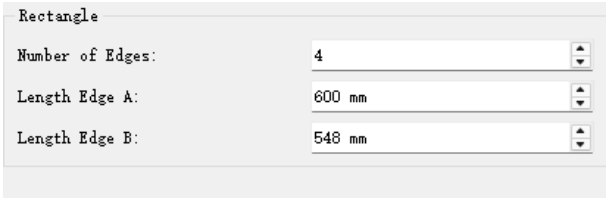

Fig. 18 – Peanut particle filling boundary conditions

The filling result is shown in Figure 17, and the Peanut particle filling boundary conditions was illustrated in Figure 18. Rotational motion was applied to the beater part. The shelling drum was given a rotation based on the actual shelling speed, tentatively set to 300 rpm, rotating counterclockwise. The housing remained stationary. Control variables were kept the same for the comparative experiment to observe the force on peanuts. The final simulation force diagrams were used to judge the rationality of the cylindrical beater.

Simulation result analysis

After the simulation ended, force line graphs and 3D force diagrams could be exported. From the line graphs (Fig. 19), it can be clearly seen that under the same other conditions, the force exerted by the cylindrical beater on the particles is relatively smaller than that of the traditional beater. The average force for the cylindrical beater is approximately 50 N, while the average maximum force for the traditional flat beater on peanuts is approximately 65 N. This also indicates that the cylindrical beater performs better in the simulation. Regarding the force on peanuts, the cylindrical beater can better reduce the force experienced by the peanut while achieving the force required for shelling, reducing peanut damage and better protecting the kernel, thus better meeting the technical requirements of shelling.

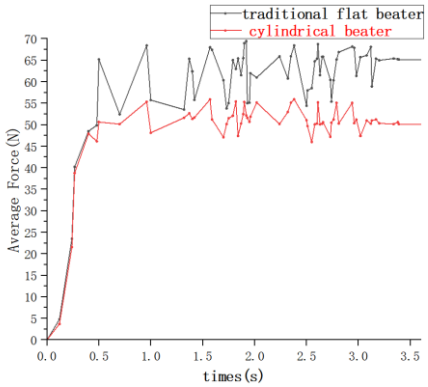

Fig.19 – EDEM simulation force diagram for cylindrical beat and traditional flat beat

Simultaneously, from the 3D schematic diagrams, it can be seen that under a single beater in the traditional beater shelling process, the number of particles experiencing the maximum force is greater than with the cylindrical beater. This indirectly indicates that the traditional beater is more likely to cause peanut stress to exceed the limit probability compared to the cylindrical beater. Specific simulation results are shown in Figure 20.

Fig. 20 – 3D force schematic for cylindrical beater and traditional flat beater

RESULTS

Following theoretical analysis, field experiments were conducted at Qingdao Wolong Peanut Machinery Co., Ltd. using machined prototype components (see Figures 19). Qinghua Y14 peanuts were selected as test material. Literature review identified drum speed and concave sieve clearance as the most influential parameters on shelling performance. Excessive rotational speed causes kernel damage, while insufficient speed reduces shelling efficiency. Similarly, improper sieve clearance either compromises shelling effectiveness or increases kernel breakage. Consequently, single-factor and orthogonal experiments were designed to determine optimal parameter combinations for final performance validation.

Single-factor experiment

Prior to the multi-factor orthogonal experiment, single-factor testing was conducted to determine appropriate parameter ranges and their individual effects on shelling rate and damage rate, with primary drum speed, primary concave sieve clearance (7-13 mm), and secondary concave sieve clearance (5-11 mm) selected as experimental factors based on preliminary analysis of peanut dimensions and mechanical behavior under idealized working conditions.

$$mv^2 - 0 = F\Delta S \quad (6)$$

$$v = n\pi \frac{D}{60} \quad (7)$$

m-mass of a single peanut, [N];

v-linear speed at the outer edge of the drum beater, [m/s];

n- drum speed, [N];

D-drum diameter, [mm];

F- impact force of the drum beater on the peanut, [N];

Δs- relative displacement of the peanut under the impact of the drum beater, [N].

Shelling condition: the force on the peanut must be greater than the shell breaking force but less than the kernel damaging force.

The shelled peanut pods and unshelled pods were collected and weighed. Damaged shelled pods were selected from the shelled output and weighed. The experimental indicators, shelling rate and damage rate, were calculated and analyzed statistically.

Shelling rate formula:

$$w_1 = \frac{M_{all} - M_1}{M_{all}} \quad (8)$$

M_{all}-shelled: total mass of shelled pods, [kg];

M_1 -unshelled: total mass of unshelled pods, [kg];

W_1 -shelling rate, [%].

Damage rate formula:

$$W_S = \frac{M_S}{M_{all}} \quad (9)$$

W_S - damage rate, [%];

M_S - mass of damaged kernels, [kg];

M_{all} - total mass of shelled pods, [kg].

Based on calculations, the required drum speed for Qinghua Y14 is approximately 280~320 rpm, Subsequently, single-factor experiments were conducted for each factor within its corresponding value range. The factor level table and experimental results are shown in the figures 21 below.

Table 6

Single-factor experiment range table

Drum Speed r/min	Primary Concave Sieve Gap/mm	Secondary Concave Sieve Gap/mm
280	5	4
300	7	6
320	9	8
340	11	10
360	13	12

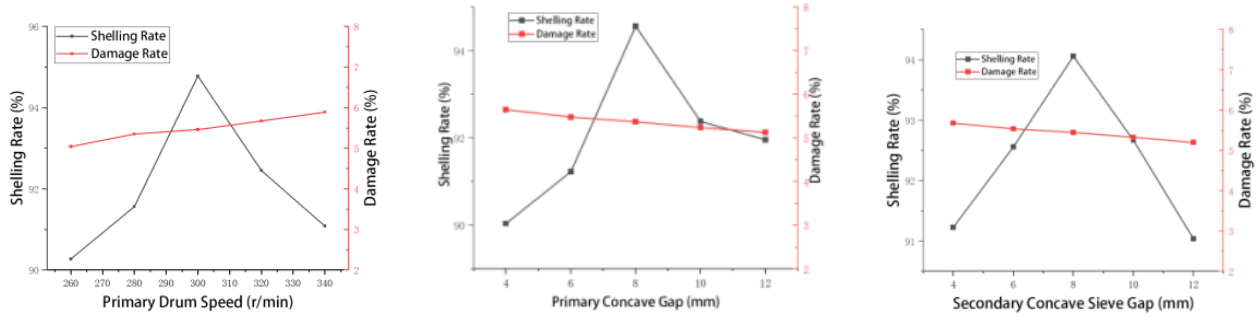

Fig. 21 –The factor experimental results

Patterns and underlying mechanisms of these parameters on peanut shelling performance (shelling rate and damage rate) were systematically revealed: as drum speed increases, the shelling rate decreases while the damage rate rises, due to excessive impact forces that easily damage kernels during shelling; the effect of the concave sieve gap is more complex, with the shelling rate initially increasing and then decreasing as the gap widens, while the damage rate consistently declines—an overly small gap leads to excessive compression

and high damage rates, a moderate gap achieves effective shelling force with controlled damage, and an excessively large gap results in insufficient impact force, reducing shelling efficiency, a pattern also observed in the secondary shelling process. In summary, this experimental phase confirms that drum speed and sieve gap are two critical yet interdependent parameters for achieving "efficient shelling with low kernel damage," providing a clear basis for subsequent multi-factor orthogonal experiments and systematic parameter optimization.

Three-factor, three-level experiment

After completing the single-factor experiments, a three-factor, three-level orthogonal experiment was conducted. The primary shelling drum speed (A), primary shelling concave sieve gap (B), and secondary shelling concave sieve gap (C) were still determined as experimental factors. In the table,“-1”: represents the "low level" or "low value" of the factor,“0”: represents the "middle level" or "center value" of the factor,“1”: represents the "high level" or "high value" of the factor. The experimental indicators were shelling rate and damage rate. The coding table and experimental results are shown below:

Table 7

Experiment coding table

Code	-Experimental Factors		
	Primary Drum Speed (min)	Primary Concave Gap (mm)	Secondary Concave Gap (mm)
-1	270	7	5
0	300	10	8
1	330	13	11

Table 8

Experimental results

Exp. No.	Factors			Experimental Indicators	
	A	B	C	Shelling Rate	Damage Rate
1	-1	-1	0	95.65	5.28
2	1	-1	0	95.14	5.59
3	-1	1	0	95.47	5.31
4	1	1	0	94.19	5.33
5	-1	0	-1	95.45	5.21
6	1	0	-1	95.29	5.47
7	-1	0	1	96.87	5.35
8	1	0	1	94.86	5.47
9	0	-1	-1	96.43	5.45
1	0	1	-1	95.69	5.35
1	0	-1	1	96.56	5.47
1	0	1	1	96.41	5.42
1	0	0	0	98.32	4.92
1	0	0	0	98.24	4.94
1	0	0	0	98.32	4.90
1	0	0	0	98.57	4.96
1	0	0	0	98.27	4.92

Variance analysis of the experimental results was performed using Design-Expert 13.0 software. The variance analysis results are shown in the table below.

Table 9

Variance analysis table

Indicator	Variance Source	Sum of Squares	DF	Mean Square	F- Value	P-value	
	Model	31.97	9	3.55	258.46	＜0.0001	Significant
	A	1.96	1	1.96	142.60	＜0.0001	

Indicator	Variance Source	Sum of Squares	DF	Mean Square	F- Value	P-value	
Shelling Rate	B	0.5101	1	0.5101	37.11	0.0005**	
	C	0.4232	1	0.4232	30.79	0.0009**	
	AB	0.1482	1	0.1482	10.78	0.0134*	
	AC	0.8556	1	0.8556	62.25	＜0.0001	
	BC	0.0870	1	0.0870	6.33	0.0400*	
	A^2	15.90	1	15.90	1156.72	＜0.0001	
	B^2	6.99	1	6.99	508.36	＜0.0001	
	C^2	2.58	1	2.58	187.92	＜0.0001	
	Residual	0.0962	7	0.0137			
	Lack of Fit	0.0277	3	0.0092	0.5390	0.6805	not -
	Pure Error	0.0685	4	0.0171			
	Cor Total	32.07	16				
Damage Rate	Model	0.8787	9	0.0976	194.99	＜0.0001**	Significant
	A	0.0630	1	0.0630	125.85	＜0.0001**	
	B	0.0180	1	0.0180	36.05	0.0005**	
	C	0.0060	1	0.0060	13.21	0.0084**	
	AB	0.0210	1	0.0210	41.99	0.0003**	
	AC	0.0049	1	0.0049	9.79	0.0167*	
	BC	0.0006	1	0.0006	1.25	0.3008	
	A^2	0.1701	1	0.1701	339.73	＜0.0001**	
	B^2	0.2600	1	0.2600	519.28	＜0.0001**	
	C^2	0.2548	1	0.2548	508.88	＜0.0001**	
	Lack of Fit	0.0035	7	0.0005			
	Pure Error	0.0014	3	0.0005	0.9135	0.5100	not significant
	Pure Error	0.0021	4	0.0005			
	Cor Total	0.8822	16				

Note：**indicates highly significant influence (P < 0.01); * indicates significant influence (0.01 < P < 0.05)*

Based on the regression analysis and variance analysis results, after eliminating non-significant influencing factors and interaction effects, the regression equations for peanut shelling rate (y_1) and peanut damage rate (y_2) are:

$$\begin{cases} y_1 = -128.12522 + 1.34150A + 3.28917B + 2.84689C - 0.002139AB - 0.005139AC + 0.016389BC - 0.002159A^2 - 0.143139B^2 - 0.087028C^2 \\ y_2 = 25.49372 - 0.119875A - 0.337500B - 0.324971C - 0.000806AB - 0.000389AC + 0.001389BC + 0.000223A^2 + 0.027611B^2 + 0.027333C^2 \end{cases} \quad (???)$$

To more intuitively represent the relationship between experimental factors and indicators, response surface plots were created using Origin software, as shown in the figure 22:

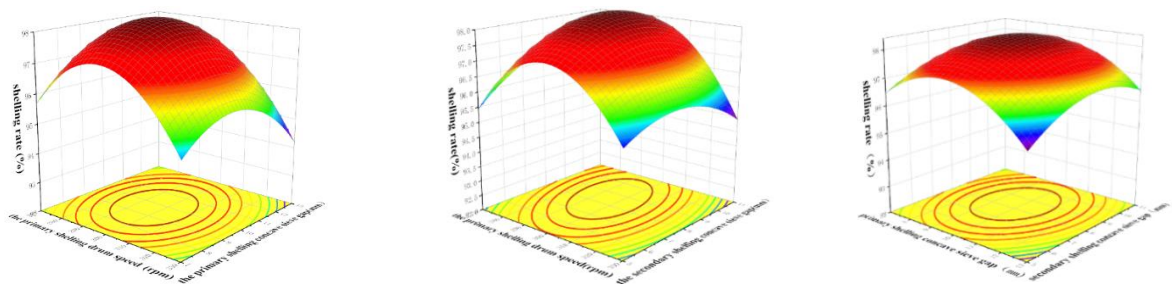

(a) (b) (c)

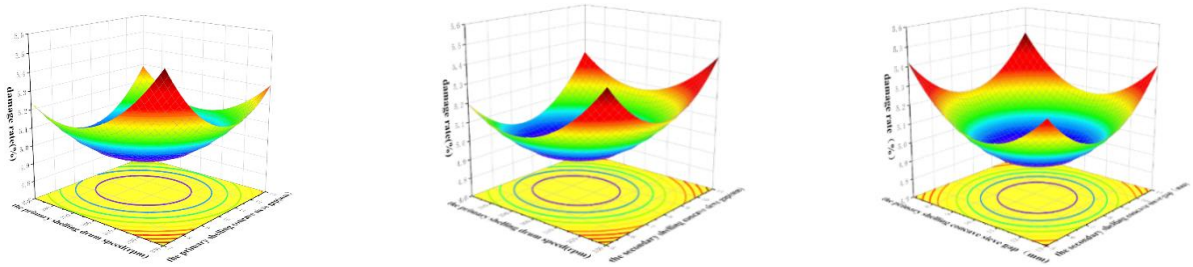

(e) (f) (g)

Fig. 22 –Response surface plots

Regression analysis and three-dimensional response surface diagrams demonstrate that the shelling rate exhibits a characteristic pattern of initial increase followed by decrease with rising parameter values, where drum speed proves to be the most influential factor, followed by primary concave sieve clearance and then secondary clearance. In contrast, the damage rate shows an inverse trend of initial decrease then increase under the same parametric variations, with the secondary sieve clearance displaying the strongest impact, the primary clearance having moderate effect, and drum speed being the least influential. Based on the optimization principle of maximizing shelling rate while minimizing damage rate, constraint conditions and objective functions were established to determine optimal operational parameters.

This analysis reveals the variation patterns under multi-parameter coupling effects and provides a theoretical basis for equipment configuration.

$$\begin{cases} \max y_1(A,B,C) \\ \min y_2(A,B,C) \end{cases} \quad \text{s.t.} \quad 270\text{rpm} \le A \le 330\text{rpm} \quad 7\text{mm} \le B \le 13\text{mm} \quad 5\text{mm} \le C \le 11\text{mm} \qquad (10)$$

The optimization module of Design-Expert software was employed for optimization calculations. From the optimization results, a reasonable parameter combination was selected: a primary shelling drum speed of 302 rpm, a primary shelling concave sieve gap of 10 mm, and a secondary shelling concave sieve gap of 8 mm. Under these parameters, the peanut shelling rate reached 98.28%, which represents an improvement compared to similar devices reported in the literature (Diao et al., 2013) where shelling rates typically range from 92% to 96%. Simultaneously, the peanut pod damage rate was controlled at 4.93%, outperforming most existing designs where damage rates are generally >6%.

Using this optimized parameter set, three validation experiments were conducted. The measured peanut shelling rate and peanut pod damage rate were 98.06% and 4.98%, respectively. The measured values are in good agreement with the predicted ones, satisfying the relevant agronomic requirements. More importantly, the operating conditions under this optimized parameter combination correspond well with the favorable working conditions identified in the earlier Discrete Element Method (DEM) simulation (cylindrical beater, average maximum force ≈50 N). This simulated force value shows a reasonable correlation with the average shelling force of approximately 40 N measured in single-peanut mechanical compression tests: the simulated force is about 1.25 times the experimental shelling force. This difference reflects the dynamic loading effects arising from particle collisions and complex motions within the simulation. It confirms that the DEM model can effectively predict and optimize the mechanical performance of the mechanism qualitatively, providing a theoretical basis for reducing the actual shelling force and minimizing damage during operation.

CONCLUSIONS

This study developed a dual-cylinder pneumatic circulation peanut sheller. Theoretical analysis identified the key operational parameters (primary drum speed and primary-secondary concave sieve clearances). An orthogonal experimental design, combined with EDEM simulation and significance analysis using the shelling rate and damage rate as evaluation metrics, determined the optimal parameter combination: the primary drum speed of 302 rpm, the primary concave sieve clearance of 10 mm, and the secondary concave sieve clearance of 8 mm. Field tests demonstrated excellent performance, achieving a shelling rate of 98.06%, a damage rate of 4.98%, and good operational reliability, meeting operational requirements.

ACKNOWLEDGEMENT

This research was supported by the Collaborative Innovation Center for Shangdong's Main crop Production Equipment and Mechanization(SDXTZX-10),the Key Research and Development Program Project of Shandong Province (2025TSGCCZZB0199), National Key Research and Development Program Project (Grant No. 2023YFD200100403).

REFERENCES

[1] Butts, C. L., & Lamb, M. C. (2016). Peanut curing and postharvest operations. In: Peanuts: Genetics, Processing, and Utilization (AOCS Monograph Series on Oilseeds). *AOCS Press*, Urbana, Illinois, USA.

[2] Chen, Y. Q., Wang, J. N., Hu, Z. C., Wang, H. O., Xie, H. X (2014). Structure optimization and experiment of bar concave for peanut sheller (花生脱机栅条凹板结构优化与试验). *Transactions of the Chinese Society of Agricultural Engineering*, Vol.30, No.07, pp.30 - 37. Beijing, China.

[3] Chen, Y., Li, M., Zhang, F., Zhang, X. J., Li, Y. M., Yang, Z. (2022). Design and experiment of a centrifugal-axial flow combined peanut shelling device (离心-轴流组合式花生脱壳装置设计与试验). J*ournal of Agricultural Machinery*, Vol.53, No.08, pp.155 - 164. Beijing, China.

[4] Diao, P. Y., Zhu, R. C., Hu, Z. C., Shen, J. H., Fu, J., & Xu, Y. X. (2020). Optimization and experiment of cone plate type peanut shelling device (锥盘式花生脱壳装置优化设计与试验). *Transactions of the Chinese Society for Agricultural Machinery*, Vol.51, No.10, pp.151 - 162. Beijing, China.

[5] Dowell, F. E. (1998). Automated color classification of single peanuts using real-time machine vision. *Transactions of the ASAE*, Vol.41, No.03, pp.839–844. https://doi.org/10.13031/2013.17228

[6] Hu, Z. C., Peng, B. L., Wang, H. O., Xie, H. X., Chen, Y. Q., Li, Y. Y. (2016). Research progress on damage mechanism and damage reduction technology of mechanical peanut shelling (机械脱壳花生损伤机理与减损技术研究进展). *Transactions of the Chinese Society of Agricultural Engineering*, Vol.32, No.17, pp.1–12. Beijing, China.

[7] Hu, Z. C., Peng, B. L., Xie, H. X., Chen, Y. Q., Wang, H. O. (2010). Research progress on peanut shelling technology and equipment (花生脱壳技术与装备研究进展). *Transactions of the Chinese Society of Agricultural Engineering*, Vol.26, No.S2, pp.357 - 363. Beijing, China.

[8] Kandala, C.V.K., & Nelson, S.O. (1990). Dielectric properties of in-shell and shelled peanuts at microwave frequencies. *Transactions of the ASAE*, Vol.33, No.03, pp.957–961.

[9] Li, K. (2018). Research on working mechanism and key components of peanut shelling device (花生脱壳装置工作机理及关键部件研究). *Shenyang Agricultural University*, Liaoning, China.

[10] Li, Z., Li, P., Yang, H., Yang, Q. Z., Wang, Y. X. (2020). Discrete element modeling and simulation of the dynamic behavior of peanut pods in a shelling chamber (花生荚在脱壳室中动态特性的离散元建模与仿真). *Biosystems Engineering*, Vol.193, pp.1 - 15.

[11] Lian, Z.G., Shang, S.Q., Wang, Y.Y. (2003). Analysis and research on main factors affecting the performance of peanut sheller (影响花生脱壳机性能的主要因素分析研究). *Journal of Laiyang Agricultural College*, Vol.20, No.02, pp.119 - 121. Shandong, China.

[12] Liu, Y. G., Xia, C., Wang, D. W., Li, Z. H., Wang, X. C., Chen, X. (2024). Simulation analysis and experiment of impact shelling process of peanut pods based on Hertz-Mindlin with bonding model (基于 Hertz-Mindlin with bonding 模型的花生荚果冲击脱壳过程仿真分析与试验). *Transactions of the Chinese Society of Agricultural Engineering*, Vol.55, No.02, pp.138–149. Beijing, China.

[13] Lopes, J.G.R., Moraes, C. H. S. V., de Medeiros, G. R., de Castro Melo, E., da Silva Araújo, C., de Sousa Rios, M. (2011). *Mechanical Properties of Peanut Shells. Journal of Food Engineering*, Vol.105, pp.212–218.

[14] National Bureau of Statistics. (2024). 2024 China Statistical Yearbook (2024 年中国统计年鉴). *China Statistics Press*, Beijing, China.

[15] Peng, B. L., Hu, Z. C., Xie, H. X., Chen, Y. Q., Wang, H. O. (2011). Optimization of peanut shelling process parameters based on response surface methodology (基于响应面法的花生脱壳工艺参数优化). *Transactions of the Chinese Society of Agricultural Engineering*, Vol.27, No.10, pp.25 - 30. Beijing, China.

[16] Sun, W., Wang, Y. Y., Shang, S. Q. (2007). Experimental study on shelling performance of 5HH-800 peanut sheller (5HH-800 型花生脱壳装置脱壳性能试验研究). *Journal of Agricultural Mechanization Research*, No.01, pp.116 – 118. Heilongjiang, China.

[17] Wang, H. O., Hu, Z. C., Chen, Y. Q., Peng, B. L., Xie, H. X., Zhang, Y. J. (2017). Research status and development of cleaning device for peanut sheller discharge (花生脱壳机出仁口清选装置研究现状与发展). *Transactions of the Chinese Society of Agricultural Engineering*, Vol.38, No.09, pp.63 – 69. Beijing, China.

[18] Wang, H. O., Hu, Z. C., Xie, H. X., Peng, B. L., Chen, Y. Q. (2015). Design and experiment of flexible impact peanut shelling device (柔性冲击式花生脱壳装置设计与试验). *Transactions of the Chinese Society of Agricultural Engineering*, Vol.31, No.19, pp.11 – 18. Beijing, China.

[19] Wang, X. C., Li, Z. H., Cao, X. L., Liu, Y. G., Yang, H., Xia, C. (2023). Design and parameter optimization of a low-damage peanut pod stripping device based on flexible comb-brush (基于柔性梳刷的低损伤花生果荚剥离装置设计与参数优化). *Transactions of the Chinese Society of Agricultural Engineering*, Vol.39, No.17, pp.10–20. Beijing, China.

[20] Xie, H. X., Hu, Z. C., Peng, B. L., Wang, H. O., Chen, Y. Q. (2016). Simulation and experiment of peanut shelling process based on EDEM (基于 EDEM 的花生脱壳过程仿真与试验). *Transactions of the Chinese Society for Agricultural Machinery*, Vol.47, No.01, pp.129 – 136. Beijing, China.

[21] Zhang, F. W. (2013). Working mechanism and parameter optimization of shelling elements in peanut sheller (花生脱壳元件工作机理与参数优化). *Qingdao Agricultural University*, Shandong, China.